Shape coexistence in ^{187}Au studied by laser spectroscopy

A. E. Barzakh,[1,*] D. Atanasov,[2,†] A. N. Andreyev,[3,4] M. Al Monthery,[3] N. A. Althubiti,[5,6] B. Andel,[7,8] S. Antalic,[8] K. Blaum,[2] T. E. Cocolios,[5,7] J. G. Cubiss,[3] P. Van Duppen,[7] T. Day Goodacre,[5,9,‡] A. de Roubin,[2,§] G. J. Farooq-Smith,[5,7] D. V. Fedorov,[1] V. N. Fedosseev,[9] D. A. Fink,[2,9] L. P. Gaffney,[9,10] L. Ghys,[7,11] R. D. Harding,[3,9] M. Huyse,[7] N. Imai,[12] S. Kreim,[2,9] D. Lunney,[13,‖] K. M. Lynch,[5,9] V. Manea,[2,‖] B. A. Marsh,[9] Y. Martinez Palenzuela,[7,9] P. L. Molkanov,[1] D. Neidherr,[14] M. Rosenbusch,[15] R. E. Rossel,[9,16] S. Rothe,[9,16] L. Schweikhard,[15] M. D. Seliverstov,[1] S. Sels,[7] C. Van Beveren,[7] E. Verstraelen,[7] A. Welker,[9,17] F. Wienholtz,[9,15,¶] R. N. Wolf,[2,15,#] and K. Zuber[17]

[1]*Petersburg Nuclear Physics Institute, NRC Kurchatov Institute, 188300 Gatchina, Russia*
[2]*Max-Planck-Institut für Kernphysik, Saupfercheckweg 1, 69117 Heidelberg, Germany*
[3]*Department of Physics, University of York, York YO10 5DD, England, United Kingdom*
[4]*Advanced Science Research Center, Japan Atomic Energy Agency, Tokai-mura, Japan*
[5]*The University of Manchester, School of Physics and Astronomy, Oxford Road, M13 9PL Manchester, England, United Kingdom*
[6]*Physics Department, Faculty of Science, Jouf University, Aljouf, Saudi Arabia*
[7]*KU Leuven, Instituut voor Kern en Stralingsfysica, B-3001 Leuven, Belgium*
[8]*Department of Nuclear Physics and Biophysics, Comenius University in Bratislava, 84248 Bratislava, Slovakia*
[9]*CERN, CH-1211 Geneva 23, Switzerland*
[10]*Department of Physics, University of Liverpool, Liverpool L69 7ZE, England, United Kingdom*
[11]*Belgian Nuclear Research Center SCK-CEN, Boeretang 200, B-2400 Mol, Belgium*
[12]*Center for Nuclear Study, Graduate School of Science, The University of Tokyo, Tokyo, Japan*
[13]*CSNSM-IN2P3, Université de Paris Sud, Orsay, France*
[14]*GSI Helmholtzzentrum für Schwerionenforschung GmbH, Darmstadt 64291, Germany*
[15]*Universität Greifswald, Institut für Physik, 17487 Greifswald, Germany*
[16]*Institut für Physik, Johannes Gutenberg Universität, D-55099 Mainz, Germany*
[17]*Institut für Kern und Teilchenphysik, Technische Universität Dresden, Dresden 01069, Germany*

(Received 22 April 2020; accepted 15 June 2020; published 25 June 2020; corrected 14 October 2021)

Hyperfine-structure parameters and isotope shift of the $9/2^-$ isomeric state in ^{187}Au relative to ^{197}Au for the 267.6-nm atomic transition have been measured for the first time using the in-source resonance-ionization spectroscopy technique. The magnetic dipole moment and change in the mean-square charge radius for this $9/2^-$ isomer have been deduced. The observed large isomer shift relative to the $1/2^+$ ground state in ^{187}Au confirms the occurrence of the shape coexistence in ^{187}Au proposed earlier from the analysis of the nuclear spectroscopic data and particle plus triaxial rotor calculations. The analysis of the magnetic moment supports the previously proposed $9/2^-$, $1/2^-[541]$ assignment at moderate prolate deformation for ^{187}Au^m.

DOI: 10.1103/PhysRevC.101.064321

I. INTRODUCTION

The neutron-deficient isotopes near $Z = 82$ exhibit one of the most extensive manifestations of shape coexistence known anywhere on the nuclear chart [1]. Among other experimental observables, isotope shift (IS) data provide a model-independent approach for interpretation of nuclear structure phenomena [2]. The jumps in the mean-square charge radius extracted from the IS values are directly related to differences in nuclear deformation as demonstrated by the exemplary shape staggering in the mercury nuclei ($Z = 80$) at $N =$ 100–105 [3–5].

The neighboring neutron-deficient gold isotopes ($Z = 79$) provide another example of an abrupt change in the ground-state mean-square charge radius (at $N = 107$). This jump is due to the transition from weakly oblate ($A > 186$) to strongly prolate-deformed ($A = 183$–186) shapes [6–9]. The isotope ^{187}Au$_{108}$ lies in the immediate vicinity of this jump and exhibits multiple-coexisting structures [10,11]. The ground state ($I^\pi = 1/2^+$) is believed to be weakly oblate, whereas the $I^\pi = 9/2^-$ isomer is considered as a member of the

*barzakh_ae@pnpi.nrcki.ru
†Present address: CERN, 1211, Geneva 23, Switzerland.
‡Present address: Accelerator Division, TRIUMF, Vancouver, BC, Canada V6T 2A3.
§Present address: Centre d'Etudes Nucléaires de Bordeaux-Gradignan, 19 Chemin du Solarium, CS 10120, F-33175 Gradignan, France.
‖Present address: Université Paris-Saclay, CNRS/IN2P3, IJCLab, 91405 Orsay, France.
¶Present address: Institut für Kernphysik, Technische Universität Darmstadt, 64289 Darmstadt, Germany.
#Present address: ARC Centre of Excellence for Engineered Quantum Systems, School of Physics, The University of Sydney, Sydney, NSW 2006, Australia.

$1/2^-[541]h_{9/2}$ band at a moderate prolate deformation (see Ref. [10] and references therein). However, this suggestion is nuclear-model dependent and based on a comparison of the nuclear spectroscopic data [rotational bands, relative γ-ray intensities, available values for the $B(E2)$ and $B(M1)$] with theoretical calculations in the framework of the particle plus triaxial rotor model (PTRM) [10,12]. Whilst the previously measured IS for ^{187}Au^{g} is compatible with a small deformation for this nucleus, the IS data for ^{187}Au^{m} are missing.

The aim of the present paper is to directly determine the difference in the mean-square charge radii between the ground and isomeric states in ^{187}Au and, thus, to get information on the difference in deformation of these states. Furthermore, the determination of ^{187}Au^{m} magnetic moment from the hyperfine-structure (hfs) measurement will also allow the configuration of this state to be probed.

The investigation presented in this paper is a part of our experimental campaign at the ISOLDE facility (CERN) aimed at nuclear decay and laser spectroscopy studies of the gold isotopes. Partial results were reported in Refs. [13,14].

II. EXPERIMENTAL DETAILS

The present data originate from the same experiment as described in Ref. [13]; therefore, only a short description of the experimental and fitting procedures is given here.

The gold nuclei were produced in spallation reactions induced by the 1.4-GeV proton beam with an average current up to 2.1 μA from the CERN PS Booster, impinging on a 50-g cm^{-2}-thick UC$_x$ target. The reaction products diffused out of the high-temperature target ($T \approx 2500$ K) and effused as neutral atoms into the hot cavity of the Resonance Ionization Laser Ion Source [15,16], where the gold atoms were selectively ionized, when the laser beams were frequency tuned to the three-step gold ionization scheme [17]. The ions were then extracted from the cavity using a 30-kV electrostatic potential and separated according to their mass-to-charge ratio by the General Purpose Separator (GPS) of ISOLDE [18]. Data were collected at the two mass settings of $A = 187$ and 197. The stable ^{197}Au was used as a reference isotope for the IS measurements and its spectra were recorded on a regular basis. In the case of $A = 187$ the ion beam was a mixture of the gold and more abundantly produced surface-ionized isobaric thallium ions, as the mass-resolving power of the GPS magnet was insufficient to eliminate isobaric contamination [19].

The mass-separated beam was delivered to ISOLTRAP's multireflection time-of-flight mass separator (MR-ToF MS) for the photoion current monitoring during wavelength scans. This method was chosen, due to its capability to perform background-free single-ion counting. Details of the ISOLTRAP apparatus, the ion-beam preparation, separation, and ion-counting technique were extensively covered in Refs. [20,21]. Below is a summary of the most relevant experimental settings used during the IS and hfs measurements for ^{187}Au^{m}.

Before injection into the MR-ToF MS, the GPS ion beam was processed by ISOLTRAP's buffer-gas-filled, linear, radio-frequency quadrupole cooler and buncher (RFQCB) [22]. After initial accumulation for 500 μs the ion beam was cooled

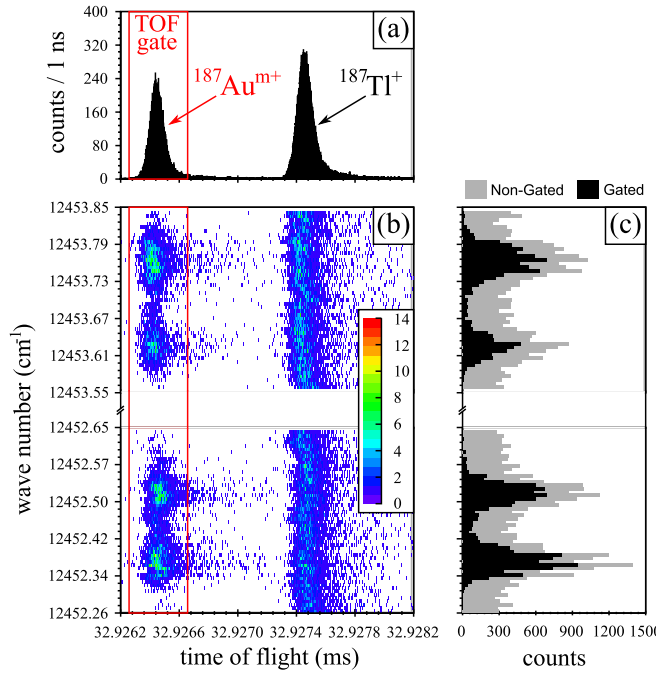

FIG. 1. (a) An example of a typical summed time-of-flight (ToF) spectrum for ^{187}Au^{m} and ^{187}Tl recorded during hfs measurements and used to establish the proper ToF gate window (red box). (b) The temporal drifts as observed in the ToF spectrum during the hfs scan. (c) Summed counts as a function of the wave number, considering the whole ToF window ("nongated") or only the ToF gate ("gated") indicated with a red box in panel (b).

for a duration of about 10 ms. The ion bunch was then extracted from the RFQCB and decelerated by a pulsed drift cavity to 3.2 keV. Afterwards the ion beam was ejected as a sequence of bunches toward the MR-ToF MS, with a typical bunch width of 60 ns. The total transport efficiency between the ISOLDE front end and the MR-ToF MS analysis detector was estimated to be 1–2%.

The isobaric separation of ^{187}Au^{m+} from the surface-ionized ^{187}Tl$^+$ was achieved by making the ion bunch to undergo 1000 revolutions between the electrostatic mirrors of the device corresponding to a trapping time of 32.876 ms (typical mass-resolving power throughout these measurements was $\approx 1.3 \times 10^5$). The ions were then extracted from the cavity and detected with an electron multiplier situated behind the MR-ToF MS, obtaining a ToF spectrum. The sum of all the recorded ToF spectra for the complete laser-frequency scan is shown in Fig. 1(a). For the IS and hfs determination a frequency-tripled titanium-sapphire laser in a narrow-band mode (bandwidth of ≈600 MHz before tripling) was scanned across the 267.6-nm atomic transition in gold ($6s\ ^2S_{1/2} \rightarrow 6p\ ^2P_{1/2}$). During the frequency scanning, ToF spectra were recorded for each frequency step.

Visualization of the laser frequency scan as a function of the total time of flight through the MR-ToF MS for ^{187}Au^{m+} and ^{187}Tl$^+$ is given in Fig. 1(b). In contrast to the laser independent ToF trace of surface-ionized ^{187}Tl, four peaks are observed for laser-ionized ^{187}Au^{m}. They correspond to the expected hfs components of the $9/2^-$ isomer (see the

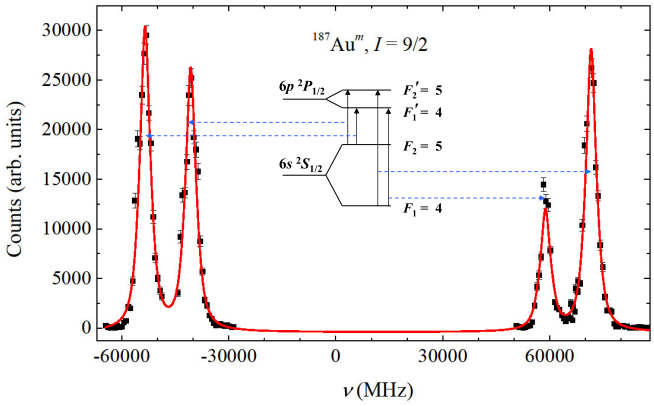

FIG. 2. An hfs spectrum of ^{187}Au^m recorded using the MR-ToF MS (black squares). The solid line depicts the Voigt-profile fit to the data. The zero point on the frequency scale corresponds to a wave number of 37 358.90 cm^{-1}. The hfs-level scheme for ^{187}Au^m is shown in the middle of the figure.

hfs-level scheme in Fig. 2). Thus, the hfs spectrum represents the variation in the photoion rate as a function of the scanned laser frequency [see Fig. 1(c)]. In order to remove the nonresonant background from the ^{187}Tl ions which would lead to the "nongated" spectrum in Fig. 1(c), the ToF gate specific to the arrival times of ^{187}Au^{m+} was applied. It is shown in Figs. 1(a) and 1(b) as a red box. As the result, a practically background-free spectrum was obtained [the "gated" spectrum in Fig. 1(c)].

III. RESULTS

Two hfs spectra for ^{187}Au^m were recorded during the experiment and an example is shown in Fig. 2. In contrast to the data shown in Fig. 1(c), in Fig. 2 the gated number of ions normalized to the measurement time at each frequency point is presented. For the $6s\ ^2S_{1/2} \rightarrow 6p\ ^2P_{1/2}$ atomic transition the positions of the hyperfine components as a function of the scanning laser frequency are determined by the formula

$$\nu^{F,F'} = \nu_0 + a_{6p}\frac{C'}{2} - a_{6s}\frac{C}{2}, \tag{1}$$

where ν_0 is the centroid frequency of the hfs, the prime symbol denotes the upper level of the atomic transition, $C = F(F+1) - I(I+1) - J(J+1)$, F is the total angular momentum of the atomic level, I and J are the nuclear spin and the angular momentum for the electronic state, respectively, and a_{nl} is the magnetic hyperfine coupling constant for the atomic level with the quantum numbers n and l. For brevity throughout the paper the indices $6s$ and $6p$ will be used to represent the $6s\ ^2S_{1/2}$ and $6p\ ^2P_{1/2}$ states, respectively.

The experimental spectra were fitted with Voigt profiles using the same method as described in Refs. [21,23]. From the result of the fit, hyperfine constants and isotope shift values $\delta\nu_{187m,197}$ were obtained:

$$a_{6s}(^{187}\mathrm{Au}^m) = 22\,480(90)\ \mathrm{MHz},$$
$$\frac{a_{6p}(^{187}\mathrm{Au}^m)}{a_{6s}(^{187}\mathrm{Au}^m)} = 0.1128(11),$$
$$\delta\nu_{187m,197} = 5380(160)\ \mathrm{MHz}.$$

A. Extraction of the change in the mean-square charge radius for ^{187}Au^m

The change in the mean-square charge radius $\delta\langle r^2\rangle_{A,A'}$ is deduced from the measured isotope shift $\delta\nu_{A,A'}$ using the relations

$$\delta\nu_{A,A'} = \delta\nu^F_{A,A'} + \delta\nu^M_{A,A'} = H(Z)F\delta\langle r^2\rangle_{A,A'} + \frac{(M^{\mathrm{NMS}} + M^{\mathrm{SMS}})(A-A')}{AA'}, \tag{2}$$

where $\delta\nu^F_{A,A'}$ and $\delta\nu^M_{A,A'}$ are the field and mass shifts, respectively, F is an electronic factor, $H(Z)$ is a factor which accounts for higher-order radial moments [24], M^{NMS} is the normal mass shift (NMS) constant ($M^{\mathrm{NMS}} = \nu/1822.9$, ν is the transition frequency), and M^{SMS} is the specific mass shift (SMS) constant.

The electronic factor $F = -43.07$ GHz fm^{-2} was taken from multiconfiguration Dirac-Fock calculations [25]. The uncertainty of the electronic factor is usually estimated as 7% [3]. It is assumed that the M^{SMS} factor for an $ns \rightarrow np$ transition is given by $M^{\mathrm{SMS}} = (0.3 \pm 0.9)M^{\mathrm{NMS}}$ [26]. For $Z = 79$ the value of $H = 0.93$ is taken from Ref. [24]. With these constants we obtain $\delta\langle r^2\rangle_{187m,197} = -0.140(4)\{14\}$ fm^2 (the statistical uncertainty is shown in parentheses; the systematic uncertainty stemming from the indeterminacy of the F and M factors is presented in the curly brackets). The isotope shift $\delta\nu_{187g,197}$ was previously measured as $\delta\nu_{187g,197} = 15\,100(210)$ MHz [6]. Combining this value with $\delta\nu_{187m,197}$ measured in the present paper, the value of isomer shift $\delta\nu_{187m,187g} = -9720(260)$ MHz was determined. Using Eq. (2) the difference between the mean-square charge radii of the ground and isomeric states in ^{187}Au was deduced: $\delta\langle r^2\rangle_{187m,187g} = 0.243(7)\{17\}$ fm^2.

The $\delta\langle r^2\rangle_{A,197}$ values for gold isotopes are plotted in Fig. 3. Literature data for $^{183-199}$Au have been taken from Refs. [6–9]. Figure 3 shows a marked increase of the ^{187}Au^m charge radius relative to that of ^{187}Au^g, which means that the former is more deformed. One can estimate the mean-squared deformation parameter $\langle\beta_2^2\rangle^{1/2}$ from the relation (see Ref. [2])

$$\langle r^2\rangle = \langle r^2\rangle_{\mathrm{DM}}\left(1 + \frac{5}{4\pi}\langle\beta_2^2\rangle\right), \tag{3}$$

where $\langle r^2\rangle_{\mathrm{DM}}$ represents the droplet-model (DM) prediction for a spherical nucleus. In Fig. 3 DM predictions [27] with constant deformation are shown, assuming $\langle\beta_2^2\rangle^{1/2}(^{197}\mathrm{Au}) = 0.11$ [6]. Using Eq. (3) and experimental values of $\delta\langle r^2\rangle_{187g,197}$ and $\delta\langle r^2\rangle_{187m,197}$ we obtain $\langle\beta_2^2\rangle^{1/2}(^{187}\mathrm{Au}^g) = 0.17(2)$ and $\langle\beta_2^2\rangle^{1/2}(^{187}\mathrm{Au}^m) = 0.23(1)$.

Thus, our results confirm the shape coexistence in ^{187}Au proposed from the earlier analysis of nuclear spectroscopic data and the PTRM calculations [10].

B. Extraction of the magnetic moment for ^{187}Au^m

In order to determine the magnetic dipole moment the standard relation was used:

$$\mu_A = \mu_{\mathrm{ref}}\frac{I_A a^A_{6s}}{I_{\mathrm{ref}} a^{\mathrm{ref}}_{6s}}[1 + {}^{\mathrm{ref}}\Delta^A(6s)] \tag{4}$$

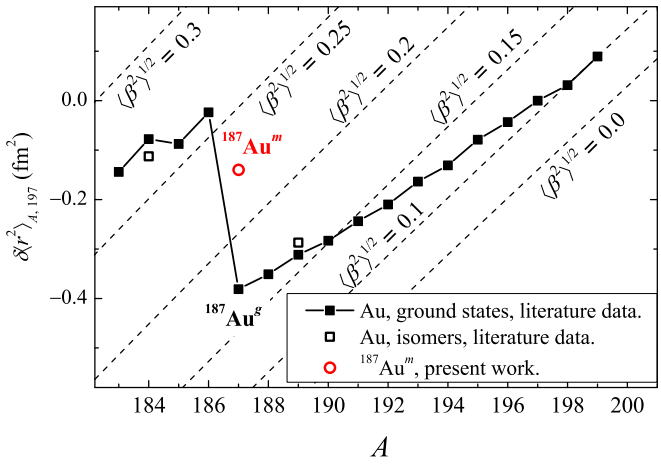

FIG. 3. Changes in the mean-square charge radii for gold isotopes relative to ^{197}Au. Open circle, present paper; squares, Refs. [6–9]. The dashed lines show the droplet model predictions with constant deformation.

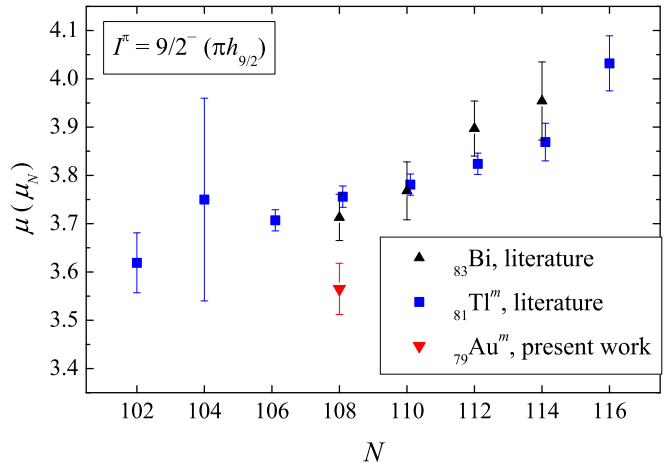

FIG. 4. Magnetic moments of the $9/2^-$ $(\pi h_{9/2})$ states in bismuth [37,38], thallium [33,34,39–41], and gold (present paper) isotopes.

where the subscript (superscript) "ref" denotes the reference isotope (^{197}Au) with known μ and a values, and $^{\rm ref}\Delta^A(6s)$ is the relative hyperfine anomaly (RHFA) stemming from the non-point-like charge and magnetization distribution inside the nucleus (see Ref. [28] and references therein). As shown in Ref. [14], the RHFA values can be deduced from the ratio of the magnetic hfs constants for different atomic states, a^A_{6s} and a^A_{6p}. This ratio depends on the nuclear spin and configuration, since different atomic states differ in sensitivity to the nuclear magnetization distribution. This change can be related to the difference of the corresponding RHFA values by introducing a differential hyperfine anomaly (DHFA) [14]:

$$ {}^{\rm ref}_{6p}\Delta^A_{6s} \equiv \frac{\left(a^{\rm ref}_{6p}/a^{\rm ref}_{6s}\right)}{\left(a^A_{6p}/a^A_{6s}\right)} - 1 = \frac{1 + {}^{\rm ref}\Delta^A(6p)}{1 + {}^{\rm ref}\Delta^A(6s)} - 1. \qquad (5)$$

With the ratio of the $6s$ and $6p$ anomalies

$$ \eta_{6s,6p} \equiv \frac{{}^{\rm ref}\Delta^A(6s)}{{}^{\rm ref}\Delta^A(6p)}, \qquad (6)$$

calculated using the advanced atomic approaches in Ref. [14], $\eta_{6s,6p} = 4.0(3)$, the RHFA value needed for the magnetic moment evaluation [Eq. (4)] is deduced from the measured DHFA:

$$ {}^{A_1}\Delta^{A_2}(6s) = \frac{{}^{A_1}_{6p}\Delta^{A_2}_{6s}}{1/\eta_{6s,6p} - 1 - {}^{A_1}_{6p}\Delta^{A_2}_{6s}}. \qquad (7)$$

With $a_{6s}(^{197}{\rm Au}) = 3049.660\,092(7)$ MHz [29], $a_{6p}(^{197}{\rm Au}) = 321.7(12)$ MHz [30], and $\mu(^{197}{\rm Au}) = 0.145\,74(4)\ \mu_N$ (data from Ref. [29] with diamagnetic correction from Ref. [31]) we obtain by Eqs. (7) and (4) $^{197}\Delta^{187m} = 0.095(16)$ and $\mu(^{187}{\rm Au}^m) = 3.529(53)\ \mu_N$.

IV. DISCUSSION

It is instructive to compare the structure of ^{187}Au^m to the well-known $9/2^-$ isomers in thallium and bismuth isotopes. The $9/2^-$ intruder isomers in $^{183-201}{\rm Tl}_{102-120}$ are considered to be weakly oblate with near constant deformation of $\beta_2 \approx -0.15$, and with the odd proton in a $9/2^-[505]h_{9/2}$ Nilsson state [32–34]. At the same time, the $9/2^-$ ground states in $^{193-209}{\rm Bi}_{110-126}$ are supposed to be nearly spherical with the relatively pure $\pi h_{9/2}$ shell-model configurations [35–37].

The magnetic moments for the $9/2^-$ bismuth [37,38] and thallium [33,34,39–41] nuclei with the same neutron number agree within the limits of uncertainties (see Fig. 4). However, the value of $\mu(^{187}{\rm Au}^m)$ measured in the present paper differs from the observed systematics (see Fig. 4), which may indicate a different structure for the long-lived $9/2^-$ state in gold as compared to thallium or bismuth. Indeed, it was shown that the PTRM calculations [10] successfully described the nuclear spectroscopic data for ^{187}Au with the assumption that the $9/2^-$ isomer in ^{187}Au is the band head of a strongly Coriolis-perturbed rotational band built on the $\pi 1/2^-[541]h_{9/2}$ Nilsson orbital, at a moderate prolate deformation. Similar ground-state bands with anomalous spin sequences were also found, e.g., in ^{183,185}Au ($5/2^-$ band head) [43,44], ^{181,183,185}Ir ($5/2^-$ band head) [45–48], ^{219}Fr ($9/2^-$ band head) [49], and ^{221}Fr ($5/2^-$ band head) [50].

As the magnetic moment is sensitive to the odd-particle configuration, we analyzed the measured $\mu(^{187}{\rm Au}^m)$ in order to check the above-mentioned assignment. In our analysis we also included the known magnetic moments of the other $\pi 1/2^-[541]h_{9/2}$ band heads in gold and francium isotopes ($5/2^-$, $1/2^-[541]$ or $9/2^-$, $1/2^-[541]$) in order to check the consistency of our approach.

The spin sequence of the unperturbed $K = 1/2$ band is determined by the relation (see Ref. [51])

$$ E_I = E_K + D[I(I+1) + a_{\rm dec}(-1)^{I+1/2}(I+1/2)], \qquad (8)$$

where D is proportional to the inverse effective moment of inertia, E_K is chosen to match the experimental band head energy, and $a_{\rm dec}$ is an energy decoupling parameter stemming from the diagonal term of the Coriolis interaction. The $a_{\rm dec}$ parameter can be determined by fitting the experimental energies of the lowest band members with Eq. (8). The magnetic moment of the $K = 1/2$ band member with spin I can be

TABLE I. A comparison between the experimental magnetic moments $\mu_{\rm expt}$ and those calculated with Eq. (9), $\mu_{\rm calc}$, for the band head levels of the $1/2^-[541]$ band in several gold and francium isotopes. The effective energy decoupling parameter, $a_{\rm dec}^{\rm eff}$, was determined from the experimental energies of the lowest band members by using Eq. (8). The effective magnetic decoupling parameter, $b_{\rm eff}$, was calculated with Eq. (10).

Isotope	I^π	$a_{\rm dec}^{\rm eff}$	$b_{\rm eff}$	$\mu_{\rm calc}$ (μ_N)	$\mu_{\rm expt}$ (μ_N)	Refs.
^{183}Au	$5/2^-$	7.2	−5.9	2.14	1.97(10)	[8,14]
^{185}Au	$5/2^-$	7.8	−6.8	2.31	2.193(61)	[6,14]
^{187}Au	$9/2^-$	8.9	−8.4	3.51	3.565(53)	Present paper
^{219}Fr	$9/2^-$	8.1	−7.3	3.29	3.13(4)	[42]
^{221}Fr	$5/2^-$	4.9	−2.9	1.57	1.57(2)	[42]

expressed as (see Ref. [52])

$$\mu = g_R I + (g_K - g_R)\frac{K^2}{I+1}[1 + (2I+1)(-1)^{I+1/2} b], \quad (9)$$

where g_R is a rotational gyromagnetic factor, g_K is an intrinsic g factor of the basic Nilsson state ($\pi 1/2^-[541]$ in our case), and b is a magnetic decoupling parameter. The parameter b is related to the energy decoupling parameter $a_{\rm dec}$ via the relation (see Ref. [53])

$$(g_K - g_R)b = -(g_l - g_R)a_{\rm dec} - \tfrac{1}{2}(-1)^l(g_s + g_K - 2g_l), \quad (10)$$

where g_l and g_s are the orbital and spin g factors, respectively.

The experimental situation when the $I^\pi = 9/2^-$ state becomes the lowest band member corresponds to a very high effective decoupling parameter, $a_{\rm dec}^{\rm eff} \approx +8$, whereas its maximal theoretical value is $a_{\rm dec} = +5$ [48]. This increase provides evidence for a supplementary perturbation coming from the nondiagonal term of the Coriolis interaction [51]. Indeed, it was shown in Ref. [51] that the Coriolis corrections to the unperturbed level energies appear as an increase in the effective decoupling parameter $a_{\rm dec}^{\rm eff}$.

Ohya *et al.* [53] suggested that the Coriolis corrections to the magnetic moments in the $\pi 1/2^-[541]$ band can also be presented as a change in the effective decoupling parameter $b_{\rm eff}$. Correspondingly, they made an estimation of $\mu(^{185}{\rm Ir})$ by Eq. (9) with an effective magnetic decoupling parameter $b_{\rm eff}$ deduced using Eq. (10) from the effective decoupling parameter $a_{\rm dec}^{\rm eff}$ of the experimental rotational band [Eq. (8)]. Using this approach, the magnetic moment of ^{185}Ir was calculated to be 2.5 μ_N, in reasonable agreement with the experimental value of 2.605(13) μ_N [53].

However, this empirical procedure was not validated by making calculations for other nuclei. We applied this procedure to $^{197}{\rm Au}^m$ and to the previously studied ^{183,185}Au and ^{219,221}Fr nuclei. In these calculations $a_{\rm dec}^{\rm eff}$ was determined from the energies of the lowest $\pi 1/2^-[541]h_{9/2}$-band members [54] with Eq. (8), and $b_{\rm eff}$ was calculated with Eq. (10), using the commonly adopted g_R and g_s factors: $g_R = Z/A$, $g_s = 0.8 g_{s,\rm free}$, and $g_K(1/2^-[541]) = 0.84$ [55] (note that usually in magnetic moment calculations for the neutron-deficient gold region two options are compared: $g_s = 0.6\, g_{s,\rm free}$ and $g_{s,\rm free}$ [9,56]; we used the mean value, $g_s = 0.8\, g_{s,\rm free}$).

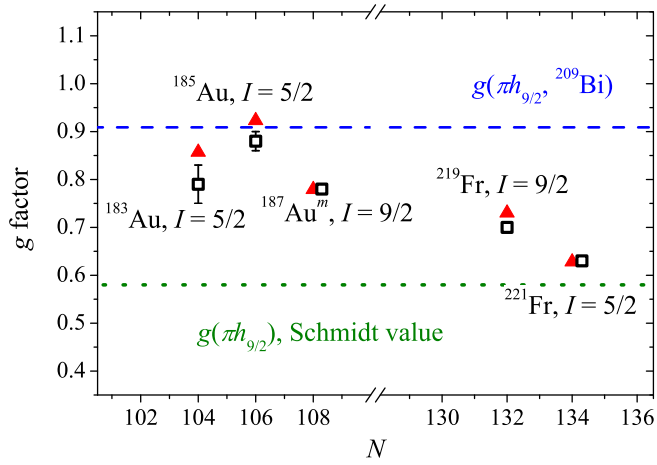

FIG. 5. A comparison of the experimental g factors (hollow squares) with those calculated using Eqs. (8)–(10) (filled triangles), at $g_R = Z/A$, $g_s = 0.8\, g_{s,\rm free}$, $g_K(1/2^-[541]) = 0.84$, and the experimental values of the decoupling parameter $a_{\rm dec}^{\rm eff}$. The dotted line shows the Schmidt value for the $\pi h_{9/2}$ state. The dashed line represents the g factor for semimagic ^{209}Bi ($I^\pi = 9/2^-$).

The results of the calculations are shown in Table I. The agreement between the calculated and experimental values is reasonable, despite the large difference in Z (79, 87), N (varying from 104 to 134), and deformation of the considered nuclei. Thus, we have shown that the empirical procedure proposed in Ref. [53] satisfactorily accounts for the magnetic moment for the band built upon the $1/2^-[541]$ Nilsson orbital.

In Fig. 5 the calculated and experimental g factors ($g = \mu/I$) are compared. All g-factor values for the presumed $1/2^-[541]$ band heads lie between the Schmidt value for the $\pi h_{9/2}$ shell and $g(^{209}{\rm Bi})$, the latter being the maximal g-factor value for the spherical nuclei with an odd proton in the $\pi h_{9/2}$ orbital. This indicates that all considered states are predominantly of the $\pi h_{9/2}$ origin. The good agreement between the calculations and experiment strongly supports the $9/2^-$, $1/2^-[541]$ assignment for $^{187}{\rm Au}^m$.

V. CONCLUSIONS

The hyperfine-structure parameters and the isotope shift relative to ^{197}Au have been measured for $^{187}{\rm Au}^m$ for the first time, using the 267.6-nm atomic transition. The magnetic dipole moment and the change in nuclear mean-square charge radius for $^{187}{\rm Au}^m$ have been deduced. The observed large $\delta\langle r^2\rangle_{187m,187g}$ value unambiguously confirms shape coexistence in ^{187}Au, as proposed from the earlier analysis of nuclear spectroscopic data and PTRM calculations [10]. The magnetic moment of $^{187}{\rm Au}^m$ has been analyzed in the framework of the empirical procedure of the magnetic moment of the $K = 1/2$ band-members estimation, implemented in Ref. [53] for ^{185}Ir. We have shown that for the bands built upon the $1/2^-[541]$ Nilsson orbital this procedure describes the g factors of the

band heads fairly well (^{183,185}Au, ^{187}Au^{m}, ^{219,221}Fr). The agreement between the calculations and experimental results supports the $9/2^-$, $1/2^-[541]$ assignment for ^{187}Au^{m}. This endorses the different nature of the $9/2^-$ states in gold (^{187}Au^{m}) and thallium or bismuth.

ACKNOWLEDGMENTS

This work was done with support from the European Union's Horizon 2020 Framework research and innovation programe under Grants No. 654002 (ENSAR2) and No. 665779 (CERN-COFUND), by RFBR according to the Research Project No. 19-02-00005, by grants from the UK Science and Technology Facilities Council (STFC), by FWO-Vlaanderen (Belgium), by Contracts No. GOA/2010/010 and No. STG/15/031 (BOF KU Leuven), by the Interuniversity Attraction Poles Programme initiated by the Belgian Science Policy Office (BriX network P7/12), by the Slovak Research and Development Agency (Contract No. APVV-18-0268), by the Slovak Grant Agency VEGA (Contract No. 1/0532/17), and by the German Federal Ministry of Education and Research (BMBF Contracts No. 05P12HGCI1, No. 05P15HGCIA, and No. 05P18HGCIA). This project has received funding through the European Union's Seventh Framework Programme for Research and Technological Development under Grants No. 262010 (ENSAR), No. 267194 (COFUND), and No. 289191 (LA^{3}NET).

[1] K. Heyde and J. L. Wood, Rev. Mod. Phys. **83**, 1467 (2011).
[2] E. W. Otten, in *Treatise on Heavy Ion Science: Volume 8: Nuclear Far From Stability*, edited by D. A. Bromley (Springer, New York, 1989), pp. 517–638.
[3] G. Ulm, S. K. Bhattacherjee, P. Dabkiewicz, G. Huber, H.-J. Kluge, T. Kühl, H. Lochmann, E.-W. Otten, K. Wendt, S. A. Ahmad, W. Klempt, R. Neugart, and ISOLDE Collaboration, Z. Phys. A **325**, 247 (1986).
[4] B. A. Marsh, T. Day Goodacre, S. Sels, Y. Tsunoda, B. Andel, A. N. Andreyev, N. A. Althubiti, D. Atanasov, A. E. Barzakh, J. Billowes, K. Blaum, T. E. Cocolios, J. G. Cubiss, J. Dobaczewski, G. J. Farooq-Smith, D. V. Fedorov, V. N. Fedosseev, K. T. Flanagan, L. P. Gaffney, L. Ghys, M. Huyse, S. Kreim, D. Lunney, K. M. Lynch, V. Manea, Y. Martinez Palenzuela, P. L. Molkanov, T. Otsuka, A. Pastore, M. Rosenbusch, R. E. Rossel, S. Rothe, L. Schweikhard, M. D. Seliverstov, P. Spagnoletti, C. Van Beveren, P. Van Duppen, M. Veinhard, E. Verstraelen, A. Welker, K. Wendt, F. Wienholtz, R. N. Wolf, A. Zadvornaya, and K. Zuber, Nat. Phys. **14**, 1163 (2018).
[5] S. Sels, T. Day Goodacre, B. A. Marsh, A. Pastore, W. Ryssens, Y. Tsunoda, N. Althubiti, B. Andel, A. N. Andreyev, D. Atanasov, A. E. Barzakh, M. Bender, J. Billowes, K. Blaum, T. E. Cocolios, J. G. Cubiss, J. Dobaczewski, G. J. Farooq-Smith, D. V. Fedorov, V. N. Fedosseev, K. T. Flanagan, L. P. Gaffney, L. Ghys, P.-H. Heenen, M. Huyse, S. Kreim, D. Lunney, K. M. Lynch, V. Manea, Y. Martinez Palenzuela, T. M. Medonca, P. L. Molkanov, T. Otsuka, J. P. Ramos, R. E. Rossel, S. Rothe, L. Schweikhard, M. D. Seliverstov, P. Spagnoletti, C. Van Beveren, P. Van Duppen, M. Veinhard, E. Verstraelen, A. Welker, K. Wendt, F. Wienholtz, R. N. Wolf, and A. Zadvornaya, Phys. Rev. C **99**, 044306 (2019).
[6] K. Wallmeroth, G. Bollen, A. Dohn, P. Egelhof, U. Krönert, M. J. G. Borge, J. Campos, A. Rodriguez Yunta, K. Heyde, C. De Coster, J. L. Wood, and H.-J. Kluge, Nucl. Phys. A **493**, 224 (1989).
[7] F. Le Blanc, J. Obert, J. Oms, J. C. Putaux, B. Roussière, J. Sauvage, J. Pinard, L. Cabaret, H. T. Duong, G. Huber, M. Krieg, V. Sebastian, J. Crawford, J. K. P. Lee, J. Genevey, and F. Ibrahim and (ISOLDE Collaboration), Phys. Rev. Lett. **79**, 2213 (1997).
[8] U. Krönert, St. Becker, G. Bollen, M. Gerber, Th. Hilberath, H.-J. Kluge, G. Passler, and ISOLDE Collaboration, Z. Phys. A **331**, 521 (1988).
[9] G. Savard, J. E. Crawford, J. K. Lee, G. Thekkadath, H. T. Duong, J. Pinard, F. Le Blanc, P. Kilcher, J. Obert, J. Oms, J. C. Putaux, B. Roussière, and J. Sauvage, Nucl. Phys. A **512**, 241 (1990).
[10] D. Rupnik, E. F. Zganjar, J. L. Wood, P. B. Semmes, and P. F. Mantica, Phys. Rev. C **58**, 771 (1998).
[11] N. Sensharma, U. Garg, Q. B. Chen, S. Frauendorf, D. P. Burdette, J. L. Cozzi, K. B. Howard, S. Zhu, M. P. Carpenter, P. Copp, F. G. Kondev, T. Lauritsen, J. Li, D. Seweryniak, J. Wu, A. D. Ayangeakaa, D. J. Hartley, R. V. F. Janssens, A. M. Forney, W. B. Walters, S. S. Ghugre, and R. Palit, Phys. Rev. Lett. **124**, 052501 (2020).
[12] S. Larsson, G. Leander, and I. Ragnarsson, Nucl. Phys. A **307**, 189 (1978).
[13] J. G. Cubiss, A. E. Barzakh, A. N. Andreyev, M. A. Monthery, N. Althubiti, B. Andel, S. Antalic, D. Atanasov, K. Blaum, T. E. Cocolios, T. D. Goodacre, R. P. de Groote, A. D. Roubin, D. V. Fedorov, V. N. Fedosseev, R. Ferrer, D. A. Fink, S. Kreim, J. Lane, V. Liberati, D. Lunney, K. M. Lynch, and V. Manea, Phys. Lett. B **786**, 355 (2018).
[14] A. E. Barzakh, D. Atanasov, A. N. Andreyev, M. Al Monthery, N. A. Althubiti, B. Andel, S. Antalic, K. Blaum, T. E. Cocolios, J. G. Cubiss, P. Van Duppen, T. D. Goodacre, A. de Roubin, Y. A. Demidov, G. J. Farooq-Smith, D. V. Fedorov, V. N. Fedosseev, D. A. Fink, L. P. Gaffney, L. Ghys, R. D. Harding, D. T. Joss, F. Herfurth, M. Huyse, N. Imai, M. G. Kozlov, S. Kreim, D. Lunney, K. M. Lynch, V. Manea, B. A. Marsh, Y. Martinez Palenzuela, P. L. Molkanov, D. Neidherr, R. D. Page, M. Rosenbusch, R. E. Rossel, S. Rothe, L. Schweikhard, M. D. Seliverstov, S. Sels, C. Van Beveren, E. Verstraelen, A. Welker, F. Wienholtz, R. N. Wolf, and K. Zuber, Phys. Rev. C **101**, 034308 (2020).
[15] V. Mishin, V. Fedoseyev, H.-J. Kluge, V. Letokhov, H. Ravn, F. Scheerer, Y. Shirakabe, S. Sundell, and O. Tengblad, Nucl. Instrum. Methods B **73**, 550 (1993).
[16] V. Fedosseev, K. Chrysalidis, T. D. Goodacre, B. Marsh, S. Rothe, C. Seiffert, and K. Wendt, J. Phys. G **44**, 084006 (2017).
[17] B. A. Marsh, V. N. Fedosseev, and P. Kosuri, Hyperfine Interact. **171**, 109 (2006).

[18] R. Catherall, W. Andreazza, M. Breitenfeldt, A. Dorsival, G. J. Focker, T. P. Gharsa, G. T. J, J.-L. Grenard, F. Locci, P. Martins, S. Marzari, J. Schipper, A. Shornikov, and T. Stora, J. Phys. G **44**, 094002 (2017).
[19] F. Kugler, Hyperfine Interact. **129**, 23 (2000).
[20] R. Wolf, F. Wienholtz, D. Atanasov, D. Beck, K. Blaum, C. Borgmann, F. Herfurth, M. Kowalska, S. Kreim, Y. A. Litvinov, D. Lunney, V. Manea, D. Neidherr, M. Rosenbusch, L. Schweikhard, J. Stanja, and K. Zuber, Int. J. Mass Spectrom. **349**, 123 (2013).
[21] J. G. Cubiss, A. E. Barzakh, M. D. Seliverstov, A. N. Andreyev, B. Andel, S. Antalic, P. Ascher, D. Atanasov, D. Beck, J. Biero, K. Blaum, C. Borgmann, M. Breitenfeldt, L. Capponi, T. E. Cocolios, U. Köster, M. Kowalska, S. Kreim, J. F. W. Lane, V. Liberati, D. Lunney, K. M. Lynch, and V. Manea, Phys. Rev. C **97**, 054327 (2018).
[22] F. Herfurth, J. Dilling, A. Kellerbauer, G. Bollen, S. Henry, H.-J. Kluge, E. Lamour, D. Lunney, R. Moore, C. Scheidenberger, S. Schwarz, G. Sikler, and J. Szerypo, Nucl. Instrum. Methods. A **469**, 254 (2001).
[23] M. D. Seliverstov, T. E. Cocolios, W. Dexters, A. N. Andreyev, S. Antalic, A. E. Barzakh, B. Bastin, J. Büscher, I. G. Darby, D. V. Fedorov, V. N. Fedosseev, K. T. Flanagan, S. Franchoo, G. Huber, M. Huyse, M. Keupers, U. Köster, Y. Kudryavtsev, B. A. Marsh, P. L. Molkanov, R. D. Page, A. M. Sjödin, I. Stefan, P. Van Duppen, M. Venhart, and S. G. Zemlyanoy, Phys. Rev. C **89**, 034323 (2014).
[24] G. Fricke and K. Heilig, in *Nuclear Charge Radii*, edited by H. Schopper (Springer, New York, 2004), pp. 1–385.
[25] A. Rosén, B. Fricke, and G. Torbohm, Z. Phys. A **316**, 157 (1984).
[26] K. Heilig and A. Steudel, At. Data Nucl. Data Tables **14**, 613 (1974).
[27] D. Berdichevsky and F. Tondeur, Z. Phys. A **322**, 141 (1985).
[28] C. Ekström, L. Robertsson, S. Ingelman, G. Wannberg, and I. Ragnarsson, Nucl. Phys. A **348**, 25 (1980).
[29] H. Dahmen and S. Penselin, Z. Phys. **200**, 456 (1967).
[30] G. Passler, J. Rikovska, E. Arnold, H.-J. Kluge, L. Monz, R. Neugart, H. Ravn, and K. Wendt, Nucl. Phys. A **580**, 173 (1994).
[31] F. D. Feiock and W. R. Johnson, Phys. Rev. **187**, 39 (1969).
[32] J. Sauvage, J. Genevey, B. Roussière, S. Franchoo, A. N. Andreyev, N. Barré, J. -F. Clavelin, H. De Witte, D. V. Fedorov, V. N. Fedoseyev, L. M. Fraile, X. Grave, G. Huber, M. Huyse, H. B. Jeppesen, U. Köster, P. Kunz, S. R. Lesher, B. A. Marsh, I. Mukha, J. Oms, M. Seliverstov, I. Stefanescu, K. Van de Vel, J. Van de Walle, P. Van Duppen, and Yu. M. Volkov, Eur. Phys. J. A **39**, 33 (2009).
[33] J. A. Bounds, C. R. Bingham, H. K. Carter, G. A. Leander, R. L. Mlekodaj, E. H. Spejewski, and W. M. Fairbank, Phys. Rev. C **36**, 2560 (1987).
[34] H. A. Schuessler, E. C. Benck, F. Buchinger, H. Iimura, Y. F. Li, C. Bingham, and H. K. Carter, Hyperfine Interact. **74**, 13 (1992).
[35] E. Coenen, K. Deneffe, M. Huyse, P. Van Duppen, and J. L. Wood, Phys. Rev. Lett. **54**, 1783 (1985).
[36] M. R. Pearson, P. Campbell, K. Leerungnavarat, J. Billowes, I. S. Grant, M. Keim, J. Kilgallon, I. D. Moore, R. Neugart, M. Neuroth, S. Wilbert, and ISOLDE Collaboration, J. Phys. G **26**, 1829 (2000).
[37] A. E. Barzakh, D. V. Fedorov, V. S. Ivanov, P. L. Molkanov, F. V. Moroz, S. Y. Orlov, V. N. Panteleev, M. D. Seliverstov, and Y. M. Volkov, Phys. Rev. C **94**, 024334 (2016).
[38] A. E. Barzakh, D. V. Fedorov, V. S. Ivanov, P. L. Molkanov, F. V. Moroz, S. Y. Orlov, V. N. Panteleev, M. D. Seliverstov, and Y. M. Volkov, Phys. Rev. C **95**, 044324 (2017).
[39] A. E. Barzakh, L. K. Batist, D. V. Fedorov, V. S. Ivanov, K. A. Mezilev, P. L. Molkanov, F. V. Moroz, S. Y. Orlov, V. N. Panteleev, and Y. M. Volkov, Phys. Rev. C **86**, 014311 (2012).
[40] A. E. Barzakh, L. K. Batist, D. V. Fedorov, V. S. Ivanov, K. A. Mezilev, P. L. Molkanov, F. V. Moroz, S. Y. Orlov, V. N. Panteleev, and Y. M. Volkov, Phys. Rev. C **88**, 024315 (2013).
[41] A. E. Barzakh, A. N. Andreyev, T. E. Cocolios, R. P. de Groote, D. V. Fedorov, V. N. Fedosseev, R. Ferrer, D. A. Fink, L. Ghys, M. Huyse, U. Köster, J. Lane, V. Liberati, K. M. Lynch, B. A. Marsh, P. L. Molkanov, T. J. Procter, E. Rapisarda, S. Rothe, K. Sandhu, M. D. Seliverstov, A. M. Sjödin, C. Van Beveren, P. Van Duppen, M. Venhart, and M. Veselský, Phys. Rev. C **95**, 014324 (2017).
[42] R. P. de Groote, I. Budinčević, J. Billowes, M. L. Bissell, T. E. Cocolios, G. J. Farooq-Smith, V. N. Fedosseev, K. T. Flanagan, S. Franchoo, R. F. Garcia Ruiz, H. Heylen, R. Li, K. M. Lynch, B. A. Marsh, G. Neyens, R. E. Rossel, S. Rothe, H. H. Stroke, K. D. A. Wendt, S. G. Wilkins, and X. Yang, Phys. Rev. Lett. **115**, 132501 (2015).
[43] M. Desthuilliers, C. Bourgeois, P. Kilcher, J. Letessier, F. Beck, T. Byrski, and A. Knipper, Nucl. Phys. A **313**, 221 (1979).
[44] C. R. Bingham, M. B. Kassim, M. Zhang, Y. A. Akovali, K. S. Toth, W. D. Hamilton, H. K. Carter, J. Kormicki, J. von Schwarzenberg, and M. M. Jarrio, Phys. Rev. C **51**, 125 (1995).
[45] E. Hagn, H. Kleebauer, and E. Zech, Phys. Lett. B **104**, 365 (1981).
[46] A. L. Allsop, V. R. Green, and N. J. Stone, Hyperfine Interact. **12**, 289 (1982).
[47] M.-G. Porquet, J. Sauvage, M. Meyer, and P. Quentin, Nucl. Phys. A **451**, 365 (1986).
[48] D. Verney, L. Cabaret, J. E. Crawford, H. T. Duong, B. Fricke, J. Genevey, G. Huber, F. Ibrahim, M. Krieg, F. Le Blanc, J. K. P. Lee, G. Le Scornet, D. Lunney, J. Obert, J. Oms, J. Pinard, J. C. Puteaux, K. Rashid, B. Roussière, J. Sauvage, V. Sebastian, and ISOLDE Collaboration, Eur. Phys. J. A **30**, 489 (2006).
[49] C. F. Liang, P. Paris, J. Kvasil, and R. K. Sheline, Phys. Rev. C **44**, 676 (1991).
[50] R. K. Sheline, Phys. Lett. B **205**, 11 (1988).
[51] S. Hjorth and H. Ryde, Phys. Lett. B **31**, 201 (1970).
[52] C. Ekström and I.-L. Lamm, Phys. Scr. **7**, 31 (1973).
[53] S. Ohya, S. Suzuki, K. Nishimura, and N. Mutsuro, J. Phys. G **14**, 365 (1988).
[54] https://www.nndc.bnl.gov/ensdf/.
[55] M. A. Cardona, A. J. Kreiner, D. Hojman, G. Levinton, M. E. Debray, M. Davidson, J. Davidson, R. Pirchio, H. Somacal, D. R. Napoli, D. Bazzacco, N. Blasi, R. Burch, D. De Acuña, S. M. Lenzi, G. Lo Bianco, J. Rico, and C. R. Alvarez, Phys. Rev. C **59**, 1298 (1999).
[56] C. Ekström, H. Rubinsztein, and P. Möller, Phys. Scr. **14**, 199 (1976).

Correction: The sixth affiliation contained errors and has been fixed.